

# Conformal Vortex Crystals

Raí M. Menezes<sup>1</sup> and Clécio C. de Souza Silva<sup>1</sup>

<sup>1</sup>*Departamento de Física, Universidade Federal de Pernambuco,  
Cidade Universitária, 50670-901 Recife-PE, Brazil*

(Dated: March 23, 2017)

We investigate theoretically globally nonuniform configurations of vortices in clean superconductors subjected to a macroscopic external force field. Our analytical and numerical simulation results demonstrate that, for suitable choices of the force field, conformal vortex crystals emerge naturally in a way as to minimize the total energy of the system. Despite being globally inhomogeneous, these ordered structures preserve the topologic order and can be mathematically mapped into a triangular lattice via a conformal transformation. We propose a simple method to engineer the potential energy profile necessary for the observation of conformal crystals of particle systems, in general, and suggest possible experiments in which conformal or quasi-conformal vortex crystals could be observed in bulk superconductors and in thin films.

Six decades after its discovery, the uniform Abrikosov lattice [1] remains as the only known ordered state of quantized vortices in type-II superconductors. Hexagonal [2–6], and in more rare instances even deformed hexagonal and square vortex lattices [7–9] are typically found in clean superconductors cooled under an applied magnetic field. In contrast, when a type-II material is cooled at zero field and only then an external field is applied, the final vortex distribution (called critical state) is typically nonuniform and highly disordered as a result of the balance between the incoming flux gradient and the random pinning forces produced by material inhomogeneities [10]. Recently, the critical state in superconducting films with periodic and graded arrays of pinning centers has been investigated in detail [11–18]. Despite the ordered nature of these pinning arrangements, the nonuniform vortex configurations reported so far are either disordered or arranged in a domain structure [11, 17].

The problem of how two-dimensional many-body systems self-organize in order to cope with an imposed density inhomogeneity or surface curvature has inspired growing interest [19–27]. A common feature in these systems is the presence of topological defects, appearing either isolated or in groups, that provide the necessary bending of lattice lines while frustrating the global orientational order [19–24, 28–30]. However, for a very limited class of planar 2D systems, namely magnetized spheres compressed by gravity [31, 32] and confined foams [33], the particles were observed to self-organize into a highly ordered, quasi-conformal crystal with a nonuniform density profile. Remarkably, these structures, dubbed gravity rainbow, can be approximately mapped into a uniform hexagonal lattice via a conformal transformation.

Mathematically, a conformal lattice in the complex  $z$  plane (representing the physical  $x$ - $y$  plane) is the result of mapping a regular, say hexagonal, lattice defined in an auxiliary  $w$  plane via a conformal (angle-preserving) transformation  $z(w) = x(u, v) + iy(u, v)$ . Since the bond angles are all preserved, the lattice in  $z$  keeps the lo-

cal hexagonal symmetry. In addition, the transformation results in a unique, generally nonuniform density distribution given by the expression  $n_z = \left| \frac{dw}{dz} \right|^2 n_w$ , with  $n_w = \text{const.}$  representing the uniform distribution in  $w$ . A relevant question is what external force field can possibly accommodate such density distribution. An approximate answer has been found only for a limited range of interaction potentials, namely inverse power laws with exponents  $k > 2$  [34]. The conditions for the observation of conformal crystals in many-body systems that do not fall on this category, such as plasmas, colloids and superconducting vortices, are still unclear.

In this letter, we demonstrate that a vortex system subjected to a suitably designed external potential can crystalize in a topologically ordered conformal lattice. Our first step towards a conformal vortex crystal (CVC) is to find what ideal external potential can accommodate particles, in general, or vortices, in particular, in a strictly conformal density profile. We approach this problem within the continuum approximation, which assumes that inter-particle spacings are smaller than any other length scale in the system. In this limit, the free-energy of a system of  $N$  particles interacting via a pair potential  $V_{\text{int}}(\mathbf{r}, \mathbf{r}')$  and subjected to an external potential  $U(\mathbf{r})$  can be expressed as a functional of the particle distribution [22]:  $\mathcal{F}[n(\mathbf{r})] = \int d\mathbf{r} n(\mathbf{r}) U(\mathbf{r}) + \frac{1}{2} \int d\mathbf{r} d\mathbf{r}' n(\mathbf{r}) V_{\text{int}}(\mathbf{r}, \mathbf{r}') n(\mathbf{r}')$ . By minimizing  $\mathcal{F}$  with respect to  $n(\mathbf{r})$ , one finds the non-local balance relation

$$U(\mathbf{r}) = - \int d\mathbf{r}' n(\mathbf{r}') V_{\text{int}}(\mathbf{r}, \mathbf{r}') + C, \quad (1)$$

where  $C$  is a constant to be determined from the number conservation condition  $\int d\mathbf{r} n(\mathbf{r}) = N$ . Notice that equation (1) can be approximated by  $U(\mathbf{r}) = -g(\mathbf{r})n(\mathbf{r})$ , with  $g(\mathbf{r}) = \int d\mathbf{r}' V_{\text{int}}(\mathbf{r}, \mathbf{r}')$ , for the cases where  $n(\mathbf{r})$  changes on a scale much larger than the characteristic length of the interaction potential. If, in addition, the interparticle force law is central,  $g$  becomes a constant and  $n(\mathbf{r})$  is essentially the negative copy of the potential.

This very simple result, which we shall refer to as local approximation, applies only when the interaction potential is short-ranged, as is the case of the vortex-vortex potential in a bulk superconductor. Otherwise, the full non-local character of Eq. (1) must be dealt with.

To be specific, we shall henceforth focus on one-dimensional external potentials,  $U(y)$ . In this case, the logarithmic map,  $z(w) = -i\ell \ln(iw/\ell)$ , is the only possible transformation that can lead to mechanically stable conformal configurations of particles interacting isotropically [34, 35]. Therefore, the required conformal density distribution in the physical  $z$  plane is  $n(y) = n_0 e^{-2y/\ell}$ , where  $n_0$  is given by number conservation condition.

Let us now apply these ideas to a system of vortices in a bulk superconductor of thickness  $d \gg \lambda$ , where  $\lambda$  is the London penetration depth. In this case, vortices interact with each other via a central pair potential given by  $V_{\text{int}}(r) = \epsilon_0 K_0(r/\lambda)$ , where  $K_0(z)$  is the zeroth-order modified Bessel function of the second kind and  $\epsilon_0 = \phi_0^2 d / 2\pi \mu_0 \lambda^2$  (with  $\phi_0$  the flux quantum and  $\mu_0$  the vacuum permeability). For large distances, this interaction decays exponentially with a characteristic length  $\lambda$ . Therefore, by further assuming that  $\ell \gg \lambda$ , the local approximation can be used, and the necessary external potential can be written as

$$U(y) = \begin{cases} -gn_0 y/\tilde{\xi}, & 0 \leq y < \tilde{\xi}, \\ -gn_0 e^{-2(y-\tilde{\xi})/\ell}, & y \geq \tilde{\xi}, \end{cases} \quad (2)$$

where the first term represents a soft-wall that confines the distribution in the  $y > 0$  region,  $g = \phi_0^2/\mu_0$ . The wall width  $\tilde{\xi}$  was chosen in a way that the maximum force exerted by the external potential,  $gn_0/\tilde{\xi}$ , is less than the vortex-antivortex unbinding force, thus avoiding violation of vortex conservation. In addition, to deal with a finite number of vortices, we assume that the potential is periodic on a length  $L$ , that is  $U(y+L) = U(y)$ , and periodic boundary conditions in the  $x$  direction, also over a length  $L$ . In all calculations using Eq. 2 we fixed  $\ell = L/\pi$ , so that the prescribed conformal transformation maps a rectangle of base  $L$  into a semiannular region. In this case, since  $\ell \ll 2L$ ,  $n_0 = 2N/[\ell(1 - e^{-2L/\ell})] \simeq 2N/\ell$ .

To find low energy configurations of the vortex system, we performed a series of Langevin dynamics simulations, following a standard simulated annealing scheme [36], of  $N = 3000$  vortices in a  $L \times 2L$  simulation box with periodic boundary conditions and  $L = 60\lambda$ . Fig. 1-(a) depicts a representative example of the most common low-energy configuration. Only a  $60\lambda \times 30\lambda$  region containing half the number of vortices is shown. As indicated by the gray shading, the lattice lines form an arch-pillar structure characteristic of a conformal lattice obtained via a logarithmic transformation of the regular hexagonal lattice. Indeed, by applying the inverse transformation,  $w(z) = -i\ell e^{iz/\ell}$ , one obtains an almost hexagonal vortex lattice in a semiannular region of the complex  $w$

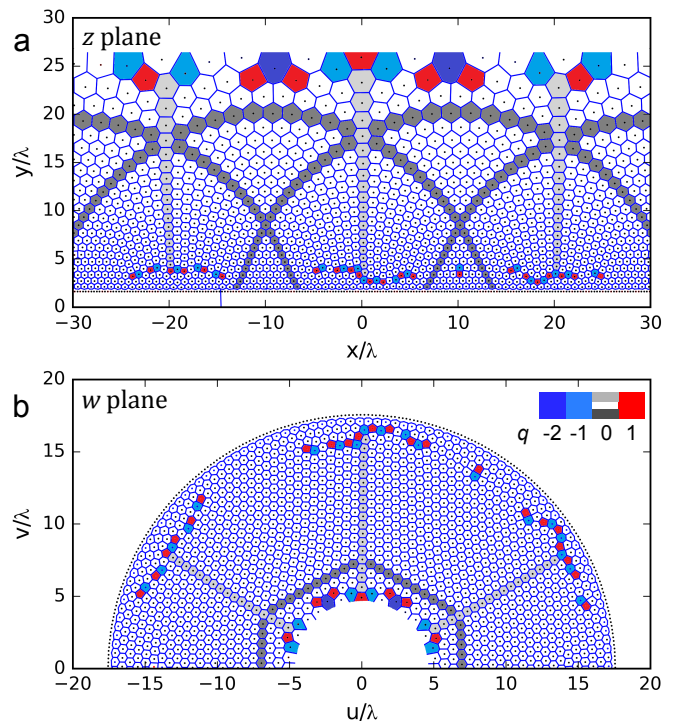


FIG. 1. (a) Typical low-energy configuration of vortices (represented by dots) in an exponential confining potential. For clarity, we disregarded the lower row of vortices in the Voronoi construction (lines). (b) Inverse conformal map of the physical  $z$  plane into the  $w$  plane (see text). The face color coding of the polygons depict the local topological charge  $q = \nu_0 - \nu$ , where  $\nu$  is the coordination number of the vortex and  $\nu_0$  the corresponding value expected for a topologically flat vortex configuration, i.e.,  $\nu_0 = 6$  (4), for a vortex in the system bulk (edge). The gray shades are guides to the eye for better identification of the arch-pillar structure of the conformal crystal.

plane, as depicted in Fig. 1-(b). As expected, the vertical pillars and arches in the  $z$  plane appear in the  $w$  plane as, respectively, radial lines forming angles of  $60^\circ$  and the sides of a regular hexagon. However, topological charges, here defined as the discrepancy in the number of first neighbors of a vortex with respect to the perfect sixfold coordination, are present. Since isolated charges costs too much energy, they typically appear in pairs (dislocations) or even larger groups. As we shall discuss later these charges play an important role in stabilizing the conformal crystal.

All other observed configurations presented a similar structure, with arches and pillars. In fact, this curved structure is so robust that it could also be observed in simulations performed with other (non-conformal) shapes of the external potential, although in these cases they are restricted to a smaller region of the system (see the Supplemental Material [37]). However, many conformal configurations were found to be broken in domains separated by prominent, transverse grain bound-

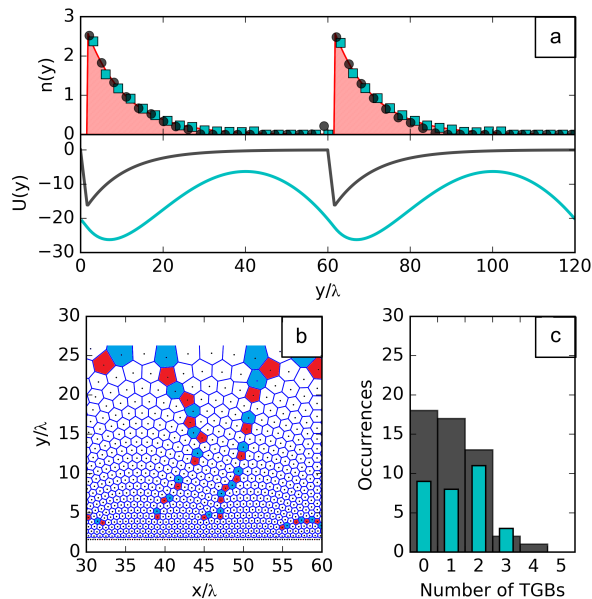


FIG. 2. (a) Top: Vortex density profiles for conformal vortex crystals in bulk samples (circles) and in thin films (squares). The area graph represents the expected exponential profile. Bottom: Potential energy profiles used in the simulations for the bulk (dark gray line) and thin-film (cyan line) cases, see Eq. (1). (b) A typical conformal configuration exhibiting transverse grain boundaries (TGBs). (c) Distribution of the configurations obtained in the simulations for a bulk sample (gray bars) and a thin film (cyan bars) according to the number of TGBs.

aries (TGBs), such as those shown in Fig. 2-(b). These dislocation lines are topologically neutral and therefore cost little energy, making it difficult to discern which configuration is closest to the ground state of the system. However, by counting the number of TGBs of 50 different realizations of the annealing procedure we can conclude that the single-domain, conformal vortex structure is the most frequent configuration and that the frequency of configurations with more than two TGBs drops fast and represents less than one third of the occurrences [see Fig. 2-(c)].

An important feature, common to all configurations irrespective of the number of TGBs, is that vortices close to the minimum of the external potential tend to form a conventional Abrikosov lattice with a principal axis aligned with the  $x$  axis. Going up in the  $y$  axis by a few vortex rows a transition to the conformal configuration can be identified. In the  $w$  plane, this depletion zone is seen as concentric vortex rings near the outer rim. While smooth at some regions, the transition is abrupt just below a pillar, where a sudden  $30^\circ$ -rotation of the principal axis can be observed. This sharp transition is delimited by high-angle grain boundaries, known as scars, which are typical defect structures found in large 2D particle systems on curved surfaces and are responsible for distributing the necessary curvature in those systems [19, 20, 27]. Here,

the net topological charge of each scar is precisely  $+1$  and is counterbalanced by a defect of charge  $-1$  near the top of each pillar. Such configuration is responsible for the deformation necessary to accommodate the conformal crystal while keeping the system globally neutral as imposed by the periodic boundary condition along the  $x$  axis. A few extra dislocations found at the top of the configuration in  $z$  (or inner rim in  $w$ ) are associated to another effect, seen in the  $w$  plane as a gentle but progressive dilation of the hexagonal cells as one approaches the inner rim. This unexpected behavior reflects the failure of the density profile to follow precisely the exponential shape [see 2-(a)], specially in the region  $y \geq 15\lambda$ , where vortex spacings become larger than  $\lambda$  and the continuum approximation breaks down.

In contrast to the above described situation, vortices in thin films interact via a long range potential, which, for  $\Lambda \equiv \lambda^2/d \rightarrow \infty$ , is essentially logarithmic,  $V(r) = \epsilon_0 \ln r$ . In addition, in order to fulfill the periodic boundary conditions, one must take into account the contribution of an infinite set of replicas for each vortex [38], which results in an effectively non-central interaction. These properties invalidate the local approximation used in the bulk case. Indeed, the calculated configuration of logarithmically interacting vortices in a potential described by Eq. 2 is non-conformal and characterized by a flat profile (see the Supplemental Material [37]). However, by numerically integrating the non-local relation, Eq. (1), using the logarithmic interaction with the appropriate boundary conditions and performing the simulated annealing scheme, conformal vortex crystals with the desired exponential density profile could be observed, see top panel of Fig. 2-(a) (a typical conformal configuration is shown in the Supplemental Material [37]). Although, the external potential for accommodating CVCs in thin films is very different from that designed for vortices in bulk samples [see bottom panel of Fig. 2-(a)], their main features are similar. However, some differences are noteworthy. For instance, the distribution of transverse grain boundaries is slightly different [Fig. 2-(c)] and suggests that a perfect conformal crystal is more difficult to achieve in thin films. On the other hand, due to the long range nature of the interactions, the density profile seems to fit better to the exponential shape predicted by the continuum theory. Indeed the mapped configurations depict a more homogeneous distribution near the inner rim in contrast to the bulk sample case.

Let us now briefly discuss the possibility of the experimental realization of a CVC. Thin films offer a more direct approach. Since these materials are unable to screen magnetic fields, one can print flux-density landscapes directly using an external magnetic texture, produced either by permanent magnets or by current-carrying wires conveniently placed on top of the superconducting film. These tools have been explored exhaustively on the mesoscopic scale as a means of manipulating vortices individ-

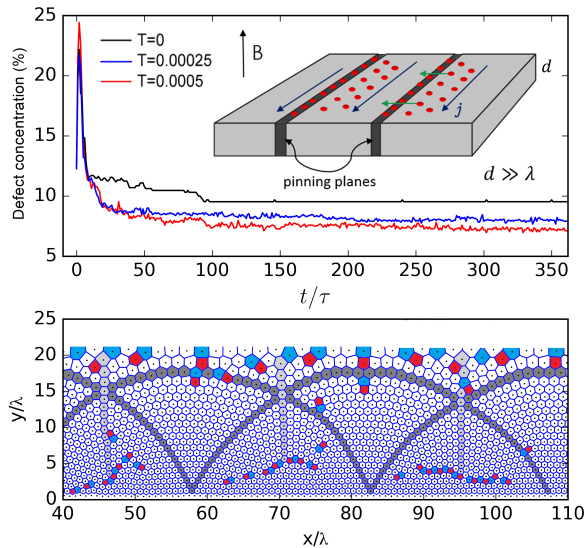


FIG. 3. Inset: schematic representation of a superconducting crystal containing parallel pinning walls (dark gray regions) where vortices (red dots) are strongly pinning and act as a dam preventing other vortices to pass through. The current density  $\mathbf{j}$  is applied in a way that the induced Lorentz force pushes the vortices in the clean regions against the vortex barriers. Top: concentration of topological defects in the vortex system as a function of time (in units of  $\tau = 30\eta\lambda^2/\epsilon_0$ ) after a current density, applied parallel to the pinning walls, is turned on at  $t = 0$  for three different temperatures (in units of  $\epsilon_0/k_B$ ). Bottom: final configuration for  $T = 0.0005\epsilon_0/k_B$  exhibiting the quasi-conformal “gravity rainbow” configuration.

ually [39–41]. In order to observe a conformal or quasi-conformal vortex crystal, one would need to design magnetic textures that resemble a smooth exponential flux decay in a length scale covering many vortex lattice spacings.

For the case of bulk superconducting samples, a possible way to induce a quasi-conformal vortex crystal is by compressing the system against a barrier using the transverse Lorentz force induced by a uniform current density applied parallel to the barrier. This concept is similar to the gravity rainbow experiment of Ref. 31. In a superconductor, vortices trapped in strong pinning planes could act as barriers for the vortices in the weak pinning regions, as suggested in the cartoon of Fig. 3. For instance, vortex rows strongly at pinned twinning planes, which are natural planar defects found in some high- $T_c$  crystals, are known to act as barriers for other vortices [42]. Alternatively, one could fabricate strong pinning planes artificially by means of lithographic and irradiation techniques [43]. To test this idea, we performed Langevin dynamics simulations of vortices in a clean superconductor with a periodic array of identical pinning potential planes modeled as  $U_p(y) = -0.8\epsilon_0 \exp(-y^2/2\xi^2)$ , with  $\xi = 0.0625\lambda$ . Two planes were placed at  $y = 0$  and  $y = 60\lambda$  and periodic boundary conditions were consid-

ered in a  $120\lambda \times 120\lambda$  simulation box containing 6.000 vortices. After a simulated annealing procedure an essentially homogeneous triangular vortex lattice was obtained, but with slightly higher vortex density at the line positions. Then, we suddenly applied a current density  $j = 0.5\epsilon_0/\lambda\phi_0$  much smaller than the depinning current ( $j_{dp} \simeq 0.5\epsilon_0/\xi\phi_0$ ), thus guaranteeing a static final configuration of the vortices. The vortices were observed to quickly compress into a linear profile, while generating a large amount of defects, and thereupon healed progressively until finally stabilizing into a quasi-conformal configuration, as the one shown in Fig. 3 (see also the supplementary video [37]). This self-organization process was observed to accelerate with the addition of small thermal fluctuations, which provide the defects with enhanced mobility allowing them to redistribute and eventually annihilate. The time evolution of the defect concentration for three different temperatures as well as the final configuration for  $T = 0.0005\epsilon_0/k_B$  are shown in Fig. 3, top panel. It is important to mention that in a real sample the healing of defects could be compromised by the ubiquitous material disorder, which tends to force the vortex system into a glassy state. However, in weak pinning superconductors, these states are characterized by a dilute distribution of topological defects that can be healed by e.g. thermal fluctuations, gentle ac shaking or a combination of both [36].

In conclusion, we have provided theoretical evidences that superconducting vortices, either in bulk materials or in thin films, can self-organize into highly ordered conformal crystals when subjected to a suitable external potential. We proposed a simple model for anticipating the external potential necessary for accommodating conformal crystals for any given interaction potential, including long-range interacting systems. As such, we expect that the results presented here also apply to other confined systems of interacting objects, e.g. colloids, plasmas and vortices in Bose-Einstein condensates. In addition, this study can be easily extended to other kinds of macroscopic confinement, such as potentials with circular symmetry. In contrast to the case of unidirectional confinement considered in the present work, a whole set of different conformal crystals could be stabilized by suitable choices of radial confinement. In this case, an accurate computation of the appropriate external potential is essential to discern the possible conformal structures.

## ACKNOWLEDGEMENTS

We thank L.R.E. Cabral and A.V. Silhanek for stimulating discussions and useful suggestions. This work was supported by the Brazilian Agencies FACEPE, under the grant Nos. APQ-2017-1.05/12 and APQ-0198-1.05/14, and CNPq.

- 
- [1] A. Abrikosov, Sov. Phys. JETP **5**, 1174 (1957).
  - [2] U. Essmann and H. Träuble, Physics letters A **24**, 526 (1967).
  - [3] H. Träuble and U. Essmann, Journal of Applied Physics **39**, 4052 (1968).
  - [4] H. F. Hess, R. B. Robinson, R. C. Dynes, J. M. Valles, and J. V. Waszczak, Phys. Rev. Lett. **62**, 214 (1989).
  - [5] D. Bishop, P. Gammel, *et al.*, Science **255**, 165 (1992).
  - [6] M. R. Eskildsen, M. Kugler, S. Tanaka, J. Jun, S. M. Kazakov, J. Karpinski, and O. Fischer, Phys. Rev. Lett. **89**, 187003 (2002).
  - [7] Y. De Wilde, M. Iavarone, U. Welp, V. Metlushko, A. E. Koshelev, I. Aranson, G. W. Crabtree, and P. C. Canfield, Phys. Rev. Lett. **78**, 4273 (1997).
  - [8] T. Riseman, P. Kealey, E. Forgan, A. Mackenzie, L. Galvin, A. Tyler, S. Lee, C. Ager, D. M. Paul, C. Aegerter, *et al.*, Nature **396**, 242 (1998).
  - [9] C. E. Sosolik, J. A. Stroschio, M. D. Stiles, E. W. Hudson, S. R. Blankenship, A. P. Fein, and R. J. Celotta, Phys. Rev. B **68**, 140503 (2003).
  - [10] C. P. Bean, Phys. Rev. Lett. **8**, 250 (1962).
  - [11] A. V. Silhanek, J. Gutierrez, R. B. G. Kramer, G. W. Ataklti, J. Van de Vondel, V. V. Moshchalkov, and A. Sanchez, Phys. Rev. B **83**, 024509 (2011).
  - [12] V. Misko and F. Nori, Physical Review B **85**, 184506 (2012).
  - [13] M. Motta, F. Colauto, W. Ortiz, J. Fritzsche, J. Cuppens, W. Gillijns, V. Moshchalkov, T. Johansen, A. Sanchez, and A. Silhanek, Applied Physics Letters **102**, 212601 (2013).
  - [14] D. Ray, C. O. Reichhardt, B. Jankó, and C. Reichhardt, Physical review letters **110**, 267001 (2013).
  - [15] Y.-L. Wang, M. Latimer, Z.-L. Xiao, R. Divan, L. Ocola, G. Crabtree, and W.-K. Kwok, Physical Review B **87**, 220501 (2013).
  - [16] S. Guénon, Y. Rosen, A. C. Basaran, and I. K. Schuller, Applied Physics Letters **102**, 252602 (2013).
  - [17] D. Ray, C. Reichhardt, and C. O. Reichhardt, Physical Review B **90**, 094502 (2014).
  - [18] Y. Wang, L. Thoutam, Z. Xiao, B. Shen, J. Pearson, R. Divan, L. Ocola, G. Crabtree, and W. Kwok, Physical Review B **93**, 045111 (2016).
  - [19] A. Bausch, M. Bowick, A. Cacciuto, A. Dinsmore, M. Hsu, D. Nelson, M. Nikolaides, A. Travesset, and D. Weitz, Science **299**, 1716 (2003).
  - [20] W. T. Irvine, V. Vitelli, and P. M. Chaikin, Nature **468**, 947 (2010).
  - [21] A. Koulakov and B. Shklovskii, Physical Review B **57**, 2352 (1998).
  - [22] A. Mughal and M. Moore, Physical Review E **76**, 011606 (2007).
  - [23] Z. Yao and M. Olvera de la Cruz, Phys. Rev. Lett. **111**, 115503 (2013).
  - [24] M. Cerkaski, R. G. Nazmitdinov, and A. Puente, Phys. Rev. E **91**, 032312 (2015).
  - [25] M. Terrones, A. R. Botello-Méndez, J. Campos-Delgado, F. López-Urías, Y. I. Vega-Cantú, F. J. Rodríguez-Macías, A. L. Elías, E. Munoz-Sandoval, A. G. Cano-Márquez, J.-C. Charlier, *et al.*, Nano Today **5**, 351 (2010).
  - [26] A. A. Pacheco Sanjuan, M. Mehboudi, E. O. Harriss, H. Terrones, and S. Barraza-Lopez, ACS nano **8**, 1136 (2014).
  - [27] C. Negri, A. L. Sellerio, S. Zapperi, and M. C. Miguel, Proceedings of the National Academy of Sciences **112**, 14545 (2015).
  - [28] L. R. E. Cabral, B. J. Baelus, and F. M. Peeters, Physical Review B **70**, 144523 (2004).
  - [29] A. Azadi and G. M. Grason, Phys. Rev. Lett. **112**, 225502 (2014).
  - [30] A. Azadi and G. M. Grason, Phys. Rev. E **94**, 013003 (2016).
  - [31] P. Pierański, in *Phase transitions in soft condensed matter*, edited by T. Riste and D. Sherington (Springer, New York, 1989) pp. 45–48.
  - [32] F. Rothen, P. Pieranski, N. Rivier, and A. Joyet, European journal of physics **14**, 227 (1993).
  - [33] W. Drenckhan, D. Weaire, and S. Cox, European journal of physics **25**, 429 (2004).
  - [34] F. Rothen and P. Pierański, Physical Review E **53**, 2828 (1996).
  - [35] K. W. Wojciechowski and J. Klos, Journal of Physics A: Mathematical and General **29**, 3963 (1996).
  - [36] B. Raes, C. C. de Souza Silva, A. V. Silhanek, L. R. E. Cabral, V. V. Moshchalkov, and J. Van de Vondel, Phys. Rev. B **90**, 134508 (2014).
  - [37] See Supplemental Material at ??? for additional simulation results and a video.
  - [38] N. Grønbech-Jensen, International Journal of Modern Physics C **7**, 873 (1996).
  - [39] D. J. Morgan and J. B. Ketterson, Phys. Rev. Lett. **80**, 3614 (1998).
  - [40] M. Lange, M. J. V. Bael, Y. Bruynseraede, and V. V. Moshchalkov, Phys. Rev. Lett. **90**, 197006 (2003).
  - [41] C. C. de Souza Silva, A. V. Silhanek, J. Van de Vondel, W. Gillijns, V. Metlushko, B. Ilic, and V. V. Moshchalkov, Phys. Rev. Lett. **98**, 117005 (2007).
  - [42] I. Maggio-Aprile, C. Renner, A. Erb, E. Walker, and Ø. Fischer, Nature **390**, 487 (1997).
  - [43] S. S. Banerjee, A. Soibel, Y. Myasoedov, M. Rappaport, E. Zeldov, M. Menghini, Y. Fasano, F. de la Cruz, C. J. van der Beek, M. Konczykowski, and T. Tamegai, Phys. Rev. Lett. **90**, 087004 (2003).